JARO 14: 813–828 (2013)
DOI: 10.1007/s10162-013-0414-z


JARO
Journal of the Association for Research in Otolaryngology

*Research Article*

# Hair Cell Generation by Notch Inhibition in the Adult Mammalian Cristae

Amber D. Slowik[1,2] and Olivia Bermingham-McDonogh[1,3]

[1]*Department of Biological Structure, University of Washington, Seattle, WA 98195, USA*

[2]*Graduate Program in Neurobiology and Behavior, University of Washington, Seattle, WA 98195, USA*

[3]*Institute for Stem Cells and Regenerative Medicine, University of Washington, Box 358056 850 Republican Street, Seattle, WA 98109, USA*

Received: 29 April 2013; Accepted: 12 August 2013; Online publication: 29 August 2013

## ABSTRACT

Balance disorders caused by hair cell loss in the sensory organs of the vestibular system pose a significant health problem worldwide, particularly in the elderly. Currently, this hair cell loss is permanent as there is no effective treatment. This is in stark contrast to nonmammalian vertebrates who robustly regenerate hair cells after damage. This disparity in regenerative potential highlights the need for further manipulation in order to stimulate more robust hair cell regeneration in mammals. In the utricle, Notch signaling is required for maintaining the striolar support cell phenotype into the second postnatal week. Notch signaling has further been implicated in hair cell regeneration after damage in the mature utricle. Here, we investigate the role of Notch signaling in the mature mammalian cristae in order to characterize the Notch-mediated regenerative potential of these sensory organs. For these studies, we used the γ-secretase inhibitor, *N*-[*N*-(3,5-difluorophenacetyl)-L-alanyl]-*S*-phenylglycine *t*-butyl ester (DAPT), in conjunction with a method we developed to culture cristae in vitro. In postnatal and adult cristae, we found that 5 days of DAPT treatment resulted in a downregulation of the Notch effectors *Hes1* and *Hes5* and also an increase in the total number of Gfi1$^+$ hair cells. Hes5, as reported by Hes5-GFP, was downregulated specifically in peripheral support cells. Using lineage tracing with proteolipid protein (PLP)/CreER;mTmG mice, we found that these hair cells arose through transdifferentiation of support cells in cristae explanted from mice up to 10 weeks of age. These transdifferentiated cells arose without proliferation and were capable of taking on a hair cell morphology, migrating to the correct cell layer, and assembling what appears to be a stereocilia bundle with a long kinocilium. Overall, these data show that Notch signaling is active in the mature cristae and suggest that it may be important in maintaining the support cell fate in a subset of peripheral support cells.

**Keywords:** inner ear, regeneration, vestibular, DAPT

## INTRODUCTION

Our sense of balance is mediated through the vestibular system, which contains multiple sensory organs composed of support cells and mechanotransducing hair cells. This includes the utricular and saccular maculae for sensing linear acceleration and the cristae for detecting rotational head movements. Balance disorders are a significant health problem worldwide with a prevalence of 21–30 % in the general population that is increased to 36–42 % in the elderly (Neuhauser et al. 2008; Gopinath et al. 2009; Mendel et al. 2010; de Moraes et al. 2011). Though many causes and factors contribute to balance disorders, there is no current effective treatment for hair cell loss either from genetic

**Electronic supplementary material** The online version of this article (doi:10.1007/s10162-013-0414-z) contains supplementary material, which is available to authorized users.

*Correspondence to*: Olivia Bermingham-McDonogh · Institute for Stem Cells and Regenerative Medicine · University of Washington · Box 358056 850 Republican Street, Seattle, WA 98109, USA.
Telephone: +206-616-4652 Fax: +206-685-1357
email: oliviab@uw.edu

disorders, drug-related ototoxicity, or age (Kroenke et al. 2000). While multiple strategies to treat hair cell loss are under investigation, regeneration would allow for replacement of already lost hair cells.

Robust regeneration is found in all nonmammalian vertebrates studied thus far, including fish, birds, and amphibians (reviewed in Warchol 2011). However, in the mammalian vestibular system, spontaneous regeneration is very limited and likely to be insufficient to restore full functionality (Tanyeri et al. 1995; Lopez et al. 1997, 1998, 2003; Forge et al. 1998; reviewed in Warchol 2011). Further manipulation is required to increase the regenerative ability of these organs.

One way to generate hair cells is through manipulation of Notch signaling, which is a pathway involved in hair cell development and differentiation. As hair cells differentiate, they express Notch ligands that bind receptors on surrounding cells. This ultimately results in a γ-secretase-mediated release of the Notch intracellular domain that translocates to the nucleus and forms a transcriptional complex that upregulates expression of effectors to prevent hair cell differentiation. This process, called lateral inhibition, establishes the mosaic-like pattern of hair cells and support cells in all of the inner ear organs including the cochlea (reviewed in Cotanche and Kaiser 2010). In the developing maculae, lateral inhibition is mediated through expression of the effectors *Hes1* and *Hes5* (Zheng et al. 2000; Zine et al. 2001). In the utricle, this Notch-mediated lateral inhibition is required into the second postnatal week and also plays a role in regeneration after damage (Wang et al. 2010; Collado et al. 2011; Lin et al. 2011; Jung et al. 2013). However, no studies have investigated Notch-mediated regeneration in the cristae.

Previously, we suggested that Notch signaling is active in the mature cristae of the mouse based on the expression of the Notch effector, Hes5 (Hartman et al. 2009). Therefore, we have carried out a series of experiments to determine if Notch is still active in the mature cristae and if it can be inhibited to generate hair cells. For these studies, we developed a method to culture cristae in vitro. Using the γ-secretase inhibitor, *N*-[*N*-(3,5-difluorophenacetyl)-L-alanyl]-*S*-phenylglycine *t*-butyl ester (DAPT), we found that Notch signaling was active in adult cristae and that supernumerary hair cells were generated by DAPT treatment. These new hair cells arose in cristae explanted from animals up to 10 weeks of age through transdifferentiation of support cells.

## METHODS

### Animals

Animal housing and care was provided by the Department of Comparative Medicine at the University of Washington. All procedures were done in compliance with the standards and protocols set forth by the University of Washington Institutional Animal Care and Use Committee. For whole mount immunostaining, cristae were collected from adult Swiss Webster mice (Harlan Laboratories). For lineage tracing experiments, proteolipid protein (PLP)/CreER;mTmG mice were generated by crossing heterozygous Plp-Cre-ER$^{T2}$ mice (Doerflinger et al. 2003; Gomez-Casati et al. 2010; Jackson Laboratories strain 005975) with homozygous ROSA-mT/mG mice (Muzumdar et al. 2007; Jackson Laboratories strain 007576). Mice were genotyped for *Cre* recombinase using DNA obtained from tail clips with the primers: forward 5′-aacattctcccaccgtcagt-3′ and reverse 5′-catttgggccagctaaaccat-3′ and for the mutant *Rosa26* allele using the primers: wild-type forward 5′-ctctgctgcctcctggcttct-3′, wild-type reverse 5′-cgaggcggatcacaagcaata-3′, and mutant reverse 5′-tcaatgggcgggggtcgtt-3′. Transgenic mice expressing GFP under the control of the *Hes5* promoter (Hes5-GFP) (Basak and Taylor 2007) were obtained from Dr. Verdon Taylor (University of Basel, Basel, Switzerland) and were used for all other experiments. Both male and female mice were used and postnatal day 0 (P0) was defined as the day of birth.

### Paint-Fill of Inner Ear

An embryonic day 14.5 (E14.5) inner ear was filled with 0.1 % white latex paint according to Morsli et al. (1998) and Kiernan (2006).

### Organotypic Cristae Cultures

Mice were euthanized according to approved procedures. Cristae were explanted from the capsule on ice in modified Hank's balanced salts solution without phenol red or sodium bicarbonate (Sigma) supplemented with 5 mM 4-(2-hydroxyethyl)-1-piperazineethanesulfonic acid (HEPES) and 200 U/mL penicillin. The semicircular canals were mechanically separated from the cristae using fine forceps, while the cupula and ampulla were left intact. The cristae were cultured in modified Dulbecco's modified Eagle's medium (DMEM)/F-12 medium [DMEM/F-12, Reh modification without L-aspartic acid, L-glutamic acid powder (US Biological) with an additional 0.3 % D-glucose, 0.8 mM GlutaMAX (Life Technologies), 0.1275 % sodium bicarbonate, 5 % fetal bovine serum (FBS), 1× N2 supplement, 1× B27 supplement, and 200 U/mL penicillin at pH 7.4], with 5 % $CO_2$ at 37 °C. Unless otherwise noted, 75 % of the media was replaced every 3 days. Cristae were cultured at the gas–liquid interface on hydrophilic PTFE cell culture inserts with 0.4 μm pores (Millipore) coated with a 2:1 mixture of 0.12 % rat tail collagen and growth factor-reduced Matrigel (BD). For pharmacological

inhibition of Notch signaling, the γ-secretase inhibitor DAPT (Calbiochem) was used at a concentration of 30 μM with an equal volume of dimethyl sulfoxide (DMSO) as a vehicle control. To induce recombination in the PLP/CreER;mTmG mice, explants were treated with 5 μM 4-hydroxytamoxifen (4-OHT; Sigma) for 2 days followed by washing prior to Notch inhibition. To assess proliferation, the thymidine analog ethynyl deoxyuridine (EdU, Life Technologies) was added to the culture media at a concentration of 5 μM. For experiments using either DAPT or EdU, 75 % of the media was replaced daily.

## Immunofluorescence

Immunostaining of whole mount cristae and cultured cristae were performed almost identically with the differences noted below. For whole mount immunostaining, capsules were removed from the head and bisected using a scalpel to isolate the vestibular system and expose the membranous labyrinth. The capsules were then fixed in cold 4 % paraformaldehyde (PFA) overnight (O/N). Cultured cristae were fixed on the culture membranes in cold 4 % PFA for 1 h. After fixation, all samples were rinsed in phosphate buffered saline (PBS), permeabilized in 0.5 % Triton-X in PBS (PBSTx) for 30 min at room temperature (RT), and then blocked in 10 % FBS in 0.5 % PBSTx for 30 min at RT. Blocking solution was used for both primary and secondary antibody solutions and 0.5 % PBSTx was used for washing. Primary antibodies were applied O/N at 4 °C and secondary antibodies were applied either O/N at 4 °C or for 3 h at RT. When applicable, Hoechst 33342 (1:10,000) was added to the secondary antibody solution. All genetically encoded fluorescent reporters, including Hes5-GFP, membrane-bound Tomato (mTomato), and membrane-bound GFP (mGFP), were visualized without additional antibody labeling.

The following primary antibodies were used: Gfi1 (guinea pig, 1:1,000, gift from Dr. Hugo J. Bellen, Baylor College of Medicine, Houston, TX, USA), Sox2 (goat, 1:400, Santa Cruz, CA, USA), Sox9 (rabbit, 1:800, Chemicon), Myosin7a (rabbit, 1:1,000, Proteus Biosciences), and Calretinin (rabbit, 1:2,000, Swant). The following secondary antibodies were used: donkey anti-guinea pig DyLight 649 (Jackson ImmunoResearch), donkey anti-goat Alexa Fluor 568 (Life Technologies), and donkey anti-rabbit Alexa Fluor 488 and 568 (Life Technologies). In addition, some samples were labeled with Phalloidin-Alexa Fluor 647 (Life Technologies). All samples were mounted in Fluoromount-G (SouthernBiotech). Whole mount cristae were mounted using 0.12 mm thick imaging spacers (Sigma).

## Quantitative RT-PCR

For the cristae cultured with DAPT or DMSO, three independent pools of cDNA were used for each condition and age. Each pool was generated using cultured cristae explanted from six to eight mice (36–48 cristae). For the analysis of uncultured cristae at various ages, only two independent pools of cDNA were used for each age. This was due to the high number of animals needed to successfully extract the RNA as each pool was generated using uncultured cristae from 12 to 14 mice (72–84 cristae). For all experiments, the pools of cristae were homogenized in 250 μL of TRIzol (Life Technologies), extracted using chloroform supplemented with 10 μg glycogen as a carrier, treated with DNase I (Qiagen), and column purified using the RNeasy Micro kit (Qiagen). cDNA was synthesized using the iScript kit (BioRad). Quantitative RT-PCR (RT-qPCR) was performed using a SYBR Green-based Master Mix (Applied Biosystems) on an ABI 7900 384- and 96- well block with TaqMan Low Density Array (Applied Biosystems). For all samples, cycle differences were normalized to the housekeeping gene, glyceraldehyde 3-phosphate dehydrogenase (*Gapdh*), and are reported as either cycle differences to GAPDH (ΔCt) or as fold changes equal to $2^{\Delta\Delta Ct}$.

The following primers were used at a final concentration of 100 nM: *Gapdh*, forward 5′-ggcattgctctcaatgacaa-3′ and reverse 5′-cttgctcagtgtccttgctg-3′; *Hes5*, forward 5′-gcaccagcccaactccaa-3′ and reverse 5′-ggcgaaggctttgctgtgt-3′; *Hes1*, forward 5′-ccgagcgtgttggggaaatac-3′ and reverse 5′-gttgatctgggtcatgcagttgg-3′; *Notch1*, forward 5′-gacaactcctacctctgcttatgcc-3′ and reverse 5′-ttact gttgcactcgttgacctcg-3′; and *eGFP*, forward 5′-gcaagctga ccctgaagttcatc-3′ and reverse 5′-tcaccttgatgccgttcttctg-3′.

## Imaging and Processing

Samples were imaged using a Nikon A1R laser scanning confocal mounted on a Nikon TiE inverted microscope. Images were taken in NIS Elements (Nikon) using either a 20× dry CFI Plan Apochromat VC objective with a numerical aperture (NA) of 0.75 or a 60× oil immersion CFI Plan Apochromat VC objective with a NA of 1.4. Unless otherwise noted, *z* stacks were taken at a step size of 0.5 μm with the 20× objective and at 0.125 μm with the 60× oil objective.

For analysis of fluorescent intensity, samples within an experiment were processed simultaneously and imaged and processed using the same intensities and settings. Maximum intensity projections were created using either NIS Elements or ImageJ. On images shown at higher magnification, blind 3D deconvolutions were performed using AutoQuant X vX2.1.1 (Media Cybernetics). Three-dimensional reconstructions and movies were created using NIS

Elements. Images for figures were compiled in Adobe Photoshop CS4. All diagrams were made by tracing either confocal images or maximum intensity projections in Adobe Illustrator CS4.

### Cell Counts, Measurements, and Statistics

Cells were counted manually in ImageJ using the standard cell counter plugin. Hair cells were counted by continuously scanning through confocal stacks taken at a $z$ interval of 0.5 μm to avoid double counting or missing cells. The hair cell counts in the control cristae are similar to what has been reported previously in adult mice with optical dissector counting (Desai et al. 2005b) and in E18.5 mice using confocal slices taken at 6 μm intervals (Fritzsch et al. 2010).

For the analysis of the fluorescence intensity of Hes5-GFP, all samples within an experiment (not across ages) were cultured, fixed, stained, imaged, and processed simultaneously using the same intensities and settings in order to preserve the integrity of the intensity comparison. Since it was therefore not appropriate to compare the absolute intensity values across ages, we showed these values as only the relative difference between the DAPT-treated cristae and their own age-matched controls. The fluorescence intensity of the entire sensory epithelium was measured in NIS Elements on maximum intensity projections as the sum fluorescence intensity per square micrometer. Since Hes5-GFP is downregulated by DAPT treatment, the sensory epithelium ROI was created by outlining the Gfi1 labeling and included the nonsensory eminentia cruciatum. The sum fluorescence intensity per square micrometer was then normalized to the average sum fluorescence intensity of six 30 $\mu m^2$ randomly placed squares outside of the sensory region (negative for both Gfi1 and Hes5).

In the lineage tracing experiments using PLP/CreER;mTmG mice, lineage traced hair cells were defined as $mGFP^+$ cells expressing the early hair cell marker Gfi1, irrespective of morphology or position. More specifically, the Gfi1 labeling had to be centered within the mGFP labeling in all dimensions to control for support cells "cupping" hair cells as they extend through the hair cell layer. In addition, lineage traced hair cells had to be distinguishable from the surrounding $GFP^+$ cells. To be counted as a lineage-traced hair cell, a cell could not exhibit ambiguity on any of these criteria, which generally resulted in the exclusion of areas of high recombination from this analysis. All $mGFP^+$ cells were analyzed in confocal stacks taken at a $z$ interval of 0.5 μm. Generally, lineage-traced hair cells expressing mGFP had decreased mTomato expression, though this was not a criterion for analysis.

Prism v5.0c (GraphPad) was used to create graphs and perform statistical analyses. The analyses used include one- or two-tailed unpaired Student's $t$ tests, one- and two-way ANOVAs, and a Pearson's correlation for the analysis of the association of the number of $GFP^+/Gfi1^+$ cells to the total $GFP^+$ cells in the sensory epithelium. The error bars of graphs depicting means are standard error of the mean (SEM). The error bars of graphs depicting differences between means are standard error of the difference (SE). SE was calculated using the following formula: SE=square root$[(SD^2/n_a)+(SD^2/n_b)]$, where SD is the standard deviation of each sample group and $n_a/n_b$ are the sizes of the two sample groups, $a$ and $b$. For one-tailed unpaired Student's $t$ tests, significance is denoted as follows: ns for $p>0.025$, * for $p\leq0.025$, ** for $p\leq0.0125$, *** for $p\leq0.00125$, and **** for $p\leq0.0001$. Otherwise, significance is denoted as: ns for $p>0.05$, * for $p\leq0.05$, ** for $p\leq0.01$, *** for $p\leq0.001$, and **** for $p\leq0.0001$. Exact $p$ values are reported for all cases where $p\geq0.0001$. Otherwise, $p$ values are reported as $p<0.0001$. For the lineage tracing and quantitative RT-PCR analyses, all cristae were analyzed. For all other experiments, only the anterior and posterior cristae are included in the analyses as one group since we did not distinguish between them.

## RESULTS

### The Cristae Ampullaris

The three cristae are situated at the bases of the three semicircular canals (Fig. 1(A,A′)). In mice, the anterior and posterior cristae are separated into two hemicristae by a hair cell-free region called the eminentia cruciatum (Fig. 1(B,D,D′); Desai et al. 2005b). The lateral crista does not have an eminentia cruciatum and is instead one continuous sensory structure (Fig. 1(C)). In addition, we found that the lateral crista had significantly fewer hair cells than anterior or posterior cristae (data not shown) and so excluded it from analyses involving hair cell counts. For this study, we used the regional boundaries defined by Desai et al. (2005b) where the central zone is the region containing the Calretinin-positive calyx afferents that innervate type I hair cells (Fig. 1(D,D′)) and the remaining sensory region is the peripheral zone. As in the other sensory organs of the inner ear, the cristae are organized into layers of hair cells ($Gfi1^+$) and support cells ($Sox2^+$, $Sox9^+$, $Hes5\text{-}GFP^+$; Fig. 1(E,F,F′)) that specifically in the cristae are folded into complex, highly three-dimensional structures. In the anterior and posterior cristae, each hemicristae is saddle-shaped (Fig. 1(F′); supplemental movie 1 in the Electronic Supplementary Material (ESM)). As reported previously, there is a subset of hair cells throughout the epithelium that also express Sox2 (yellow cells in

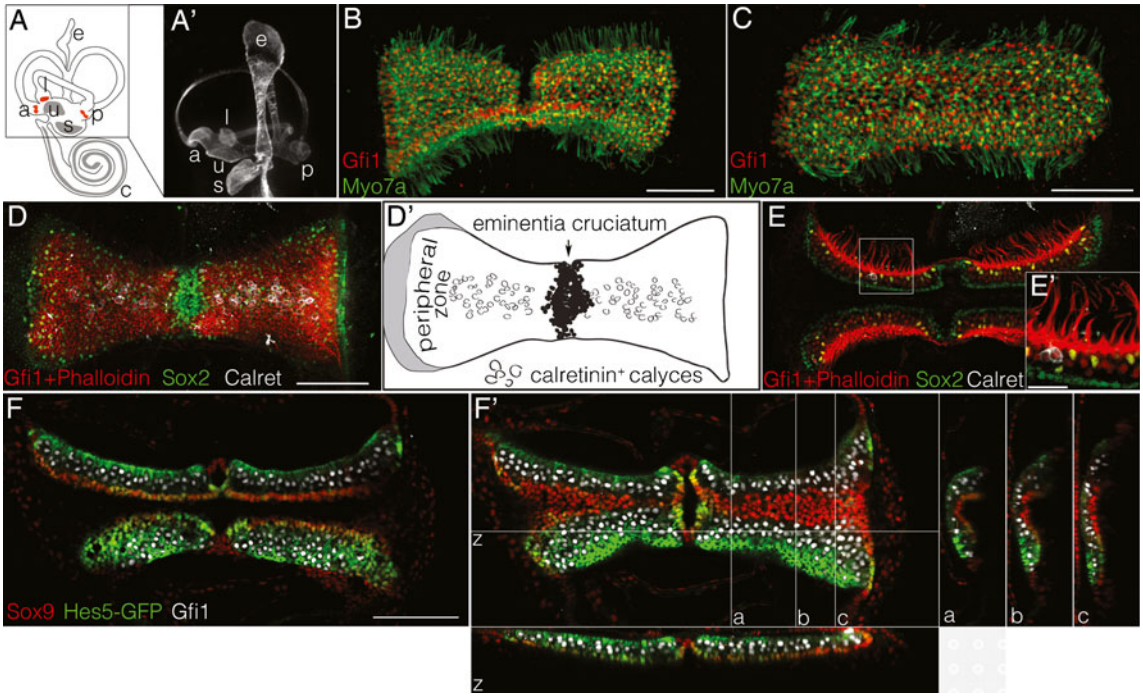


**FIG. 1.** **A**,**A′** The three cristae (*red*) are located at the bases of the semicircular canals shown in a diagram of the inner ear (**A**) and in a paint-fill of an E14.5 vestibular system (**A′**). *a* Anterior crista, *l* lateral crista, *p* posterior crista, *u* utricle, *s* saccule, *c* cochlea, *e* endolymphatic sac. **B**,**C** Maximum intensity projections of adult whole mount cristae labeled with the hair cell markers Myo7a (cytoplasmic, *green*) and Gfi1 (nuclear, *red*). The eminentia cruciatum divides the anterior (**B**) and posterior cristae into two saddle-shaped hemicristae. **C** The sensory epithelium of the lateral crista is continuous. *Scale bars* 100 μm. **D**,**D′** Sox2 (*green*) labels support cells, a subset of type II hair cells, and nonsensory cells in the planum semilunatum (*shaded gray* in *D′*) and eminentia cruciatum. The sensory epithelium contains Gfi1$^+$ hair cells (*red* nuclei) with phalloidin-stained (*red*) stereocilia bundles. The central zone was defined by the Calretinin$^+$ (*white*) calyx afferents that contact type I hair cells, while the remaining calretinin-negative region was the peripheral zone. *Scale bar* 100 μm. **E**,**E′** The layering of the support cells and hair cells of the sensory epithelium is visible in a single *z* plane depicting a cross-sectional view of the cristae from *D*. *Scale bar* in *E′* is 25 μm. **F** This layering can also be seen in cristae explanted from Hes5-GFP mice labeled with Sox9 (*red*) and Gfi1 (*white*). *Scale bar* 100 μm. **F′** The three-dimensional structure of this same cristae can be seen in *z* projections through the confocal stacks at the labeled lines (*a*, *b*, *c*, *z*). Sox9 is also expressed throughout the ampulla, which flattened onto the sensory epithelium of the cristae during mounting and culturing (*c*). *z* depth, 75.5 μm.

Fig. 1(E,E′); Hume et al. 2007; Oesterle et al. 2008). Similar to the staining seen in the utricle, this subset of cells does not appear to be innervated by Calretinin-positive calyces and is generally located closer to the apical surface of the sensory epithelium (Fig. 1(E′); Desai et al. 2005a). Together, these data suggest that these Sox2-expressing cells belong to the type II subclass of hair cells, though it is not clear whether every type II hair cell expresses Sox2.

## Organotypic Cultures of Postnatal and Adult Cristae

To test for a role of Notch signaling in the trans-differentiation of support cells in the cristae, we developed a method for maintaining cristae in vitro. In brief, cristae were dissected from the capsule (Fig. 1(A)), mechanically separated from the semicircular canals, and cultured with the ampulla intact on culture membrane inserts at the gas–liquid interface. Cristae were cultured for 5 days in vitro (DIV) and then labeled with antibodies to assess the survival of hair cells and the overall morphology of the sensory epithelium. Postnatal ages were used in addition to the mature ages for comparison purposes as the survival and plasticity of inner ear organs is generally greater at younger ages. To facilitate accurate hair cell counts, we used the nuclear hair cell marker Gfi1. Gfi1 is expressed in both the developing (Wallis et al. 2003; Hertzano et al. 2004; Yang et al. 2010) and mature (Fig. 1(B,C)) vestibular system. In the adult, counts of Gfi1$^+$ cells were nearly identical to counts with the more commonly used cytoplasmic marker, Myo7a (Hasson et al. 1995), under all culture conditions tested (Fig. 2(E)).

After 5 DIV, both postnatal (P7) and adult (P30) cristae maintained their overall morphology compared to control cristae freshly dissected from similarly staged animals (Fig. 2(B,B′,C,C′) compared to Fig. 2(A,A′)). The overall shape of the sensory

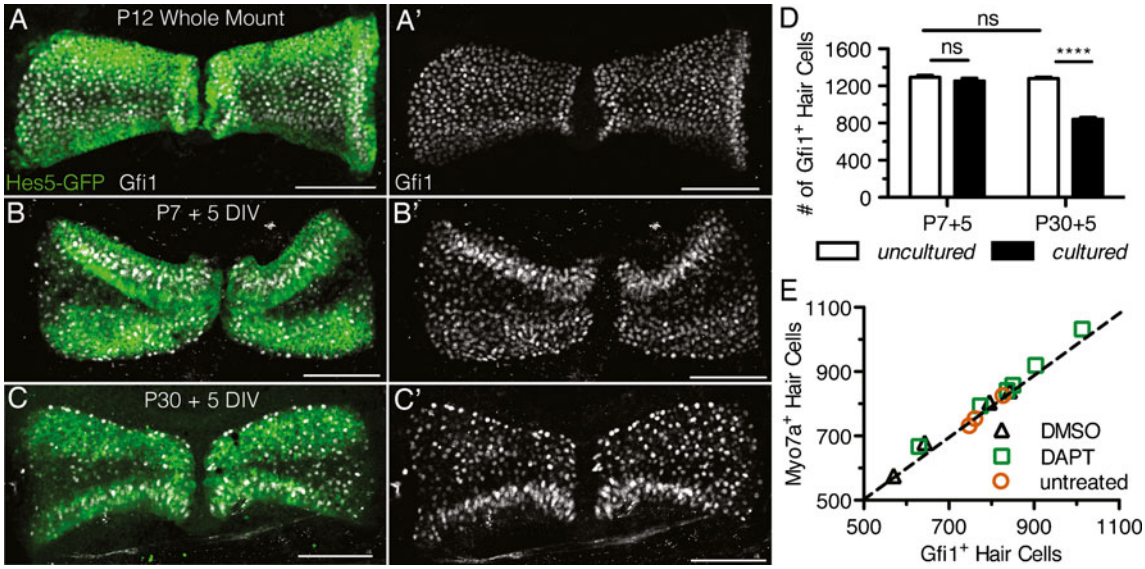


**FIG. 2.** **A**,**A′**,**B**,**B′** Maximum intensity projections of cristae explanted from P7 Hes5-GFP mice and labeled with Gfi1 (*white*) show that after 5 days in vitro (DIV) cristae maintained their overall morphology compared to uncultured littermate controls (**B**,**B′** compared to **A**,**A′**). **C**,**C′** Cristae cultured from P30 adults also maintained their normal morphology. *Scale bars* 100 μm. **D** P7+5 DIV cristae maintained similar levels of Gfi1$^+$ hair cells ($n$=11) compared to P12 littermates ($n$=9; $t$=0.9590, $df$=18, $p$=0.35), while P30+5 DIV explants had a significantly reduced number of hair cells ($n$=10) compared to P35 littermates ($n$=9; $t$=19.1571, $df$=17, $p$< 0.0001). *Error bars* depict SEM. Two-tailed unpaired Student's $t$ test where ns denotes $p$>0.05 and **** denotes $p\leq$0.0001. **E** In P30+ 5 DIV cristae, the hair cell counts obtained using an antibody to Gfi1 were comparable to those using an antibody to Myo7a regardless of culture conditions (DMSO, $n$=4, DAPT, $n$=6, untreated, $n$=3).

epithelium was maintained, including the separation of the epithelium into the two distinct hemicristae by the eminentia cruciatum. In addition, in cultures from transgenic mice expressing GFP under the *Hes5* promoter (Hes5-GFP), the expression of GFP in the peripheral zone and immunostaining with the hair cell markers Gfi1 and Myo7a (data not shown) were similar to control explants (Fig. 2(A,A′,B,B′,C,C′)). However, there was a slight difference in the appearance of the cultured cristae in maximum intensity projections. This was due to the flattening and folding of the highly three-dimensional tissue onto the culture membrane. The degree of folding varied from explant to explant, but most commonly appeared as in Figure 2(B,B′,C,C′).

In addition to morphology, we assessed the overall hair cell survival after 5 DIV at both P7 and P30 (Fig. 2(D)). In the P7 explants, nearly all the hair cells survived the 5-day culture period with 1,253.4±30.8 ($n$=11) Gfi1$^+$ hair cells in cultured explants compared with 1,291.4±22.3 ($n$= 9) in littermate controls ($t$=0.9590, $df$=18, $p$=0.35). By contrast, in the P30 explants, there was significant hair cell loss after 5 DIV with 843.5±17.2 ($n$=10) Gfi1$^+$ hair cells compared to 1,280.7±14.5 ($n$=9) in littermate controls ($t$=19.1571, $df$=17, $p$<0.0001) (Fig. 2(D)). This loss appears to be due to culture survivability and is not related to age-dependent hair cell loss as there was no significant difference in hair cell number between the P7 and P30 uncultured explants ($t$= 0.4044, $df$=16, $p$=0.69). Overall, at P30, there was a 34.1 % loss due to culture, which is consistent with that seen in other adult cultures of vestibular organs (e.g. Lin et al. 2011). Generally, this loss appeared as an overall thinning of the hair cell density throughout the sensory epithelium (Fig. 2(C′)); however, occasionally there was an almost complete loss of the hair cells in more central regions.

## Notch Signaling is Active in Adult Cristae

Previously, we suggested that Notch signaling was active in the peripheral support cells of the adult cristae based on an analysis of the Notch effector Hes5 in Hes5-GFP reporter mice and on *Hes5* expression examined by in situ hybridization (Hartman et al. 2009). To provide additional evidence that the Hes5 expression seen in the adult is a result of active Notch signaling, cristae from postnatal (P7, P12, and P14) and adult (P30) Hes5-GFP mice were explanted and treated with the γ-secretase inhibitor, DAPT to pharmacologically inhibit Notch signaling. The postnatal ages were used for comparison since the ability to generate supernumerary hair cells through Notch inhibition is lost after P12 in the utricle (Collado et al. 2011). After 5 DIV with 30 μM DAPT, the Hes5-GFP expression specific to the support cells of the peripheral zone was downregulated compared to the DMSO controls in all of the ages examined (Fig. 3(A)). In the P30 explants, there was some remaining fluores-

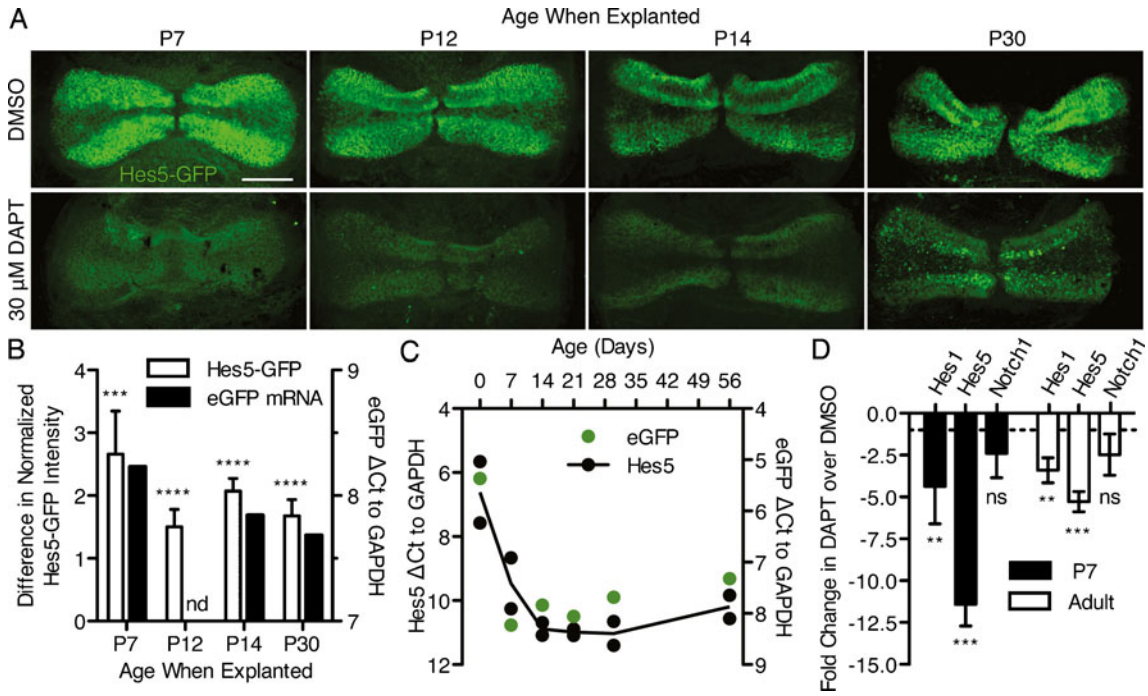


**FIG. 3.** Notch signaling was active in the postnatal and adult cristae. **A** Hes5-GFP was expressed in the support cells along the peripheral edges of the cristae at all ages in DMSO controls and was down-regulated by 30 μM DAPT after 5 DIV. *Scale bar* 100 μm. **B** Quantification of the Hes5-GFP fluorescence intensity showed significant reduction with DAPT treatment at all ages (*white bars*, *n*=[DMSO; DAPT]; P7 [10; 8], −2.66±0.69, $t$=3.868, $df$=16, $p$=0.00068; P12 [10; 12], −1.50±0.27, $t$=5.467, $df$=20, $p$<0.0001; P14 [12; 12], −2.07±0.20, $t$=10.30, $df$=22, $p$<0.0001; P30 [19; 13], −1.68±0.26, $t$=6.453, $df$=30, $p$<0.0001). *Error bars* depict SE. The difference in fluorescent intensity showed a similar trend with age as the gene expression of eGFP assayed by RT-qPCR (*black bars*; P7, 8.226; P12, no data (nd); P14, 7.840; P30, 7.682). **C** RT-qPCR analysis of uncultured cristae showed that endogenous *Hes5* (*black points*) is downregulated postnatally but maintains similar levels of expression between late postnatal and adult ages (8 weeks). Each point represents a single biological replicate, while the *black line* shows the average of the two replicates (P0, 6.613±1.356; P7, 9.463±1.124; P14, 10.884±0.280; P21, 10.988±0.143; P30, 11.025±0.530; P56, 10.198±0.511). Error on reported values is standard deviation. The expression of *eGFP* from the Hes5-GFP transgene in these same organs showed a similar trend to that of *Hes5* (*green points*; P0, 5.364; P7, 8.226; P14, 7.840; P21, 8.060; P30, 7.682; P56, 7.320). **D** RT-qPCR analysis of cristae explanted from P7 and adult (8–10 weeks) mice showed a significant reduction in *Hes1* (P7: −4.38±1.28, $t$=3.8060, $df$=4, $p$=0.0095; adult: −3.40±0.43, $t$=3.5309, $df$=4, $p$=0.012) and *Hes5* (P7: −11.42±0.75, $t$=11.4975, $df$=4, $p$=0.00016; adult: −5.28±0.35, $t$=6.7954, $df$=4, $p$=0.0012) gene expression in DAPT treated cristae over DMSO controls after 5 DIV with no change in Notch1 expression (P7: −2.38±0.85, $t$=2.0646, $df$=4, $p$=0.054; adult: −2.47±0.72, $t$=1.8732, $df$=4, $p$=0.067). *Error bars* depict SEM. One-tailed unpaired Student's $t$ test where $^{ns}p>0.025$, $^{*}p\leq0.025$, $^{**}p\leq0.0125$, $^{***}p\leq0.00125$, $^{****}p\leq0.0001$.

cent signal due to the autofluorescence of dead and dying cells, indicative of the decreased survivability of the adult explants. Quantification of the difference in Hes5-GFP fluorescence intensity between DAPT- and DMSO-treated cristae shows that this downregulation was significant at all ages examined (white bars, Fig. 3(B)). Further, the degree of this downregulation showed a similar trend with age to the expression of *eGFP* in uncultured cristae from Hes5-GFP mice assayed by RT-qPCR (black bars, Fig. 3(B)). Overall, in the uncultured cristae, it appeared that *Hes5* gene expression was highly downregulated postnatally, but remained relatively stable after P7 and into the adult ages (black circles, Fig. 3(C)). The expression of *eGFP* from the *Hes5-GFP* reporter shows an identical trend (green circles, Fig. 3(C)). In addition, RT-qPCR analysis of cristae explanted from P7 and adult (8–10 weeks) mice and cultured for 5 DIV, showed that the Notch effectors *Hes1* and *Hes5* were significantly downregulated in DAPT-treated cristae over DMSO controls, with no change in the expression of the Notch receptor, *Notch1* (Fig. 3(D)). Overall, these data show that Notch signaling is active in the adult cristae, albeit possibly at a lower level than in early postnatal animals.

## DAPT Treatment Increases Total Hair Cell Number

The presence of active Notch signaling in the adult cristae led us to hypothesize that Notch signaling may still be necessary to maintain the support cell phenotype in mature cristae and that Notch inhibition would lead to the generation of supernumerary hair cells. To test this, postnatal (P7, P12, and P14) and

adult (P30) explants were cultured for 5 DIV with 30 μM DAPT or DMSO as a vehicle control (Fig. 4). Cristae were analyzed by counting the total number of Gfi1$^+$ hair cells. This concentration of DAPT is lower than that used in similar studies in the utricle (Collado et al. 2011; Lin et al. 2011) and was chosen based on a concentration curve performed on P7 explants cultured for 5 DIV with 1, 10, or 30 μM DAPT with DMSO as a vehicle control. This is in contrast to the postnatal cochlea where 5 μM DAPT is sufficient to inhibit lateral inhibition (Hayashi et al. 2008). To determine efficacy, the difference in the total number of Gfi1$^+$ hair cells between DAPT- and DMSO-treated cristae was used. Only the explants treated with 30 μM DAPT showed a statistically significant increase in hair cell number over the DMSO controls (DMSO, 1,153±37.29 ($n$=10); 1 μM, 1,222±76.05 ($n$=3); 10 μM, 1,157±38.15 ($n$=4); 30 μM, 1,380±89.79 ($n$=7); means reported with SEM; one-way ANOVA where $F(4,20)=3.223$, $p=0.0445$ with Tukey–Kramer post-test [$\alpha=0.05$]). Overall, there was a highly statistically significant effect of DAPT on total hair cell number (Table 1). In addition, there was also a statistically significant effect of age on total hair cell number as the survivability of the explants decreased with increasing age (Fig. 2(D), Table 1). However, there was no differential effect of DAPT treatment with age as the interaction between them was not significant (Table 1). At each individual age tested, there was a significant increase in the number of hair cells in DAPT-treated cristae relative to their aged-matched controls (Table 1, Fig. 4(B)). In the P7 explants, there was a noticeable increase in the hair cell density in the region near the eminentia cruciatum (Fig. 4(A), arrows) that was accompanied by a loss of Sox9$^+$ support cells in the same regions (Fig. 5(A), arrows). In the adult explants (P30), the increase in hair cells was not as apparent in the maximum intensity projections; nevertheless, there was a consistent and statistically significant increase in the number of hair cells in the DAPT-treated explants, even at P30 (Fig. 4(B)). This increase in hair cell number was approximately the same at all of the ages tested (Table 1, Fig. 4(C)), which is consistent with the relatively stable levels of *Hes5* gene expression at these same ages (Fig. 3(C)).

These hair cell increases did not appear to be due to cell proliferation. Culturing for 5 DIV with

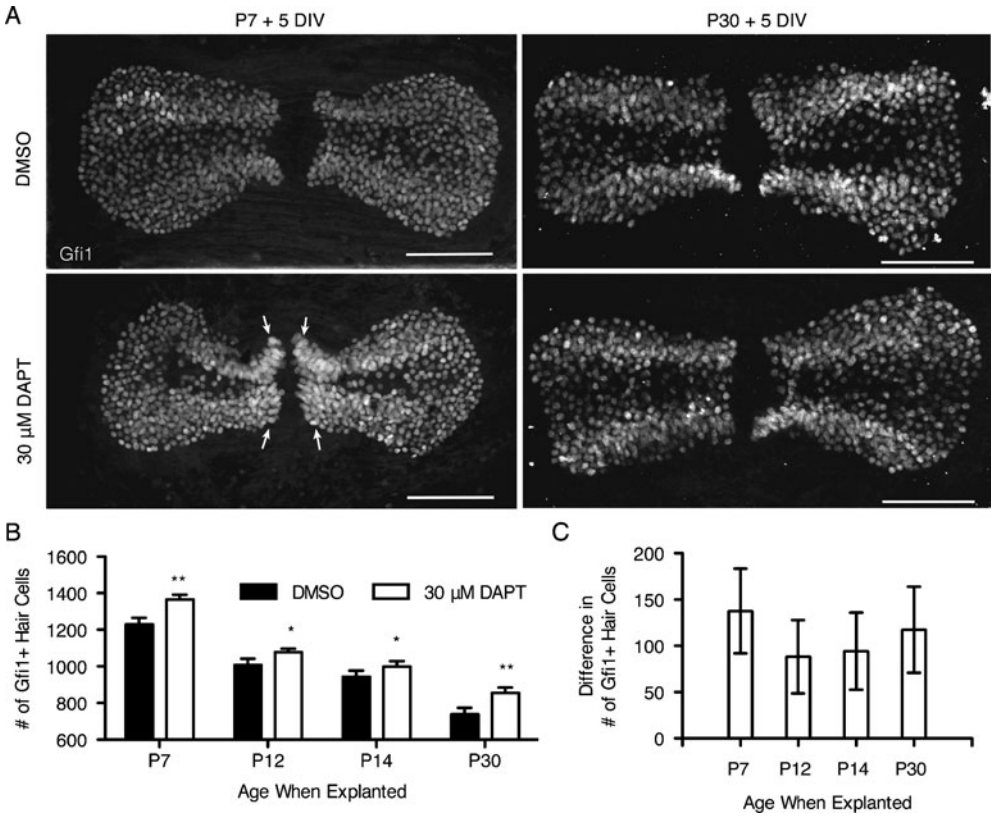


**FIG. 4.** Total hair cell number increased upon DAPT treatment in postnatal and adult cristae. **A** Maximum intensity projections of Gfi1$^+$ hair cells in explants from P7 and P30 mice after 5 DIV with 30 μm DAPT or DMSO. *Scale bars* 100 μm. *Arrows* point to regions of increased hair cell density. **B** At each age examined, the total number of Gfi1$^+$ hair cells was significantly increased in DAPT-treated cristae versus DMSO controls (Table 1). Note that the scale on the *y*-axis begins at 600. *Error bars* depict SEM. One-tailed unpaired Student's $t$ test where $^*p \leq 0.025$ and $^{**}p \leq 0.0125$. **C** The difference in hair cell number between treated and control cristae was similar at all ages. *Error bars* depict SE.

**TABLE 1**

Quantification of Gfi1$^+$ hair cells in cristae explants cultured for 5 DIV

| *Explant age and treatment* | *n* | *Mean (±SEM)* | *Difference between means (±SE)* | *p value (Df, t)*[a] |
|---|---|---|---|---|
| P7 | | | | |
| DMSO | 15 | 1,228 (±36.79) | −137.6 (±45.79) | 0.0028 |
| DAPT | 15 | 1,366 (±27.26) | | (28, 3.005) |
| P12 | | | | |
| DMSO | 15 | 996.5 (±35.37) | −88.13 (±39.5) | 0.0169 |
| DAPT | 15 | 1,085 (±17.58) | | (28, 2.231) |
| P14 | | | | |
| DMSO | 11 | 922.5 (±24.82) | −94.35 (±41.62) | 0.0176 |
| DAPT | 10 | 1,017 (±34.10) | | (19, 2.267) |
| P30 | | | | |
| DMSO | 22 | 738.9 (±35.07) | −117.3 (±46.4) | 0.0078 |
| DAPT | 19 | 856.2 (±29.01) | | (39, 2.528) |
| Two-way ANOVA | | | *F* value | *p* value |
| Effect of DAPT | | | $F_{1,114}$=21.85 | <0.0001 |
| Effect of age | | | $F_{3,114}$=92.57 | <0.0001 |
| Interaction | | | $F_{3,114}$=0.23 | 0.8722 |

*SEM* standard error of the mean, *SE* standard error of the difference

[a]*p* values from one-tailed unpaired Student's *t* tests with degrees of freedom and *t* value

continuous 5 μM EdU did not result in EdU uptake by Gfi1$^+$ hair cells in either DAPT- or DMSO-treated cristae, despite numerous EdU$^+$ cells in the surrounding nonsensory tissue (Fig. 5(B)). In addition, the majority of support cells appeared to be negative for EdU labeling based on their position in the sensory epithelium and nuclear morphology. It is still possible, however, that there was a low level of support cell proliferation, as we did not label the support cells to test for this. The data shown in Fig. 5(B) is an example of a P30 explant, though we found the same results at P7 and P14 as well. Overall, this suggests that any newly generated hair cells did not arise through proliferation, but through direct transdifferentiation.

## New Hair Cells Arise Through Transdifferentiation of Support Cells

In order to directly demonstrate that the hair cell increases we observed were due to support cell transdifferentiation and not from hair cell survival or repair, we used a lineage tracing strategy to label support cells prior to DAPT treatment (Fig. 6(A)). For these experiments, we used animals that had reached sexual maturity (8–10 weeks) as we felt that they better represented mature adults. Our analysis of *Hes5* gene expression, both with age and with DAPT treatment, suggested that Notch signaling was still active at this age (Fig. 3(C,D)). Further, the 8- to 10-week-old control cristae cultured for 7 DIV from this experiment had a similar number of Gfi1$^+$ hair cells (836.2±41.52, $n$=5) as our cultured P30+5 DIV explants (Fig. 2(D); 843.5±17.2, $n$=10). This suggests that even though the adult explants do not survive as well in culture as younger explants, their survivability does not continue to decline with age, but stabilizes between at least P30 and P56-70. To label support cells, we used PLP/CreER mice expressing an inducible *Cre* recombinase under the PLP promoter crossed to mTmG reporter mice that express mTomato prior to recombination and mGFP after *Cre*-mediated recombination (Doerflinger et al. 2003; Muzumdar et al. 2007; Gomez-Casati et al. 2010). Upon tamoxifen treatment, the support cells and Schwann cells that express the *PLP* transgene expressed GFP in a dose-dependent manner (Fig. 6(B,C,D)). By replacing the media with fresh 5 μM 4-OHT each day of the 2-day recombination period, it was possible to recombine almost all of the peripheral support cells (Fig. 6(D)). However, with this recombination efficiency, it was impossible to distinguish between a hair cell expressing mGFP and an unlabeled hair cell surrounded by support cells expressing mGFP. Using a single treatment of 5 μM 4-OHT with no media change during the 2 days of recombination, we had a lower recombination efficiency overall (Fig. 6(E,E′), with and without Gfi1). With this recombination efficiency, the morphology and layering of individual cells when viewed in single $z$ planes was clearly visible (Fig. 6(F,F′,F″), arrows indicate regions of support cell recombination, asterisk indicates a region of Schwann cell recombination). To verify that the *Cre* recombinase was not expressed in hair cells, cristae were explanted from 8- to 10-week-old PLP/CreER;mTmG mice and treated with 5 μM 4-OHT for 2 DIV to induce recombination.

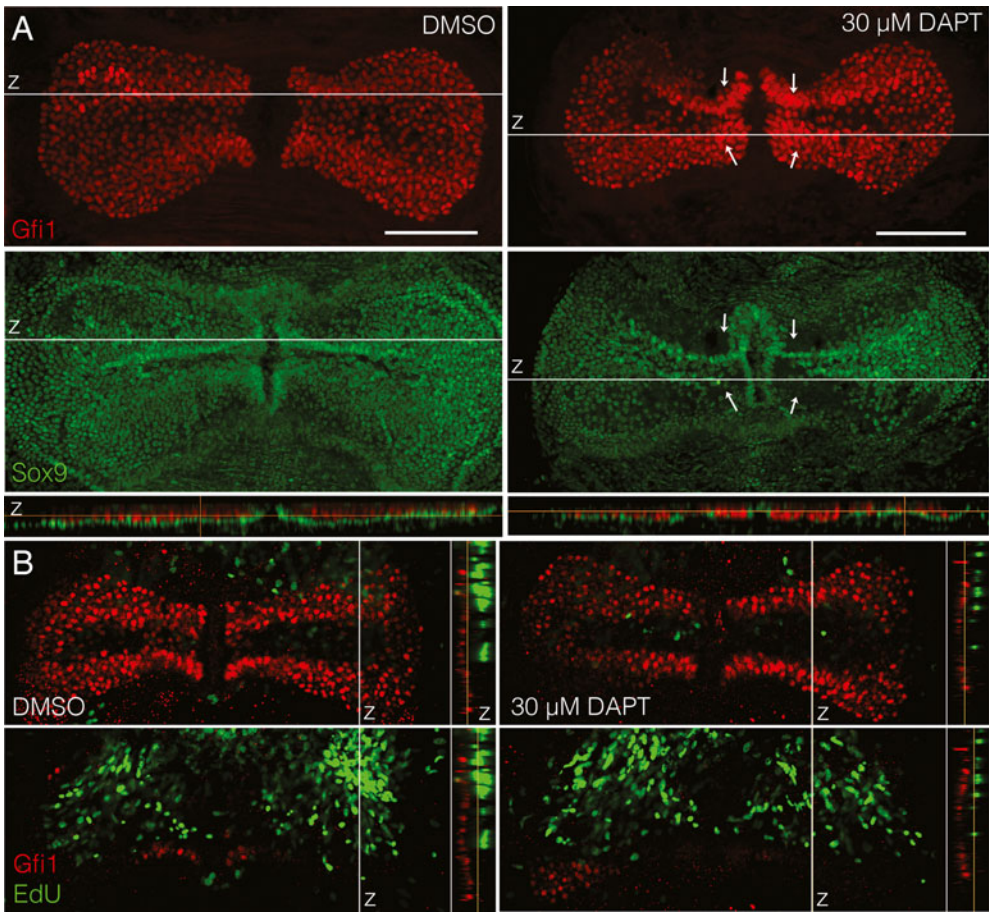


**FIG. 5.** Hair cells appear to arise through transdifferentiation of support cells without proliferation. **A** In maximum intensity projections of P7+5 DIV cristae treated with 30 μm DAPT, the Sox9$^+$ support cell layer (*green*) was disrupted near the eminentia cruciatum as compared to DMSO-treated controls where the Sox9 layer was continuous (*arrows* point to regions of increased hair cell density and decreased support cell density). This can also be seen in *z* projections through the sensory epithelium (at the *white lines*) where in controls the green support cell layer was continuous beneath the red hair cells, but in DAPT-treated cristae it was disrupted. This obvious disruption is not seen in adult explants. *Scale bars* 100 μm. **B** In P30 explants cultured for 5 DIV, hair cells did not take up EdU, despite the presence of EdU throughout the entire culture period. Cristae are shown in single slice views with labeling for Gfi1 (*red*) and EdU (*green*). *z* slice projections are shown to the *right* of the image indicating the location of the slice relative to the sensory epithelium in the *z* dimension. In both conditions, while many cells beneath the sensory epithelium were positive for EdU, no Gfi1$^+$ hair cells had EdU labeling, as indicated by the lack of yellow cells.

Recombination control cristae were fixed directly after these 2 days and analyzed. Out of nine recombination control cristae, no hair cell recombination was observed despite significant support cell recombination comparable to the number of GFP$^+$ cells in the sensory epithelium quantified in Figure 7(B).

To determine whether the additional hair cells we observed with DAPT treatment were derived from support cells, we explanted cristae from 8- to 10-week-old PLP/CreER;mTmG mice and treated them with 5 μM 4-OHT for 2 DIV to induce recombination as described above. After 2 DIV, the media was replaced with either 30 μM DAPT or DMSO as a vehicle control for an additional 5 DIV (Fig. 7(A)). Both treated and control cristae had similar rates of recombination (Fig. 7(B)). In the DMSO-treated controls there were 225.6±27.3 ($n$=18) recombined mGFP$^+$ cells in the sensory epithelium compared to 183.8±22.0 ($n$=29) mGFP$^+$ cells in the DAPT-treated cristae ($t$=1.155, $df$=45, $p$=0.25). Further, in the DAPT-treated cristae, we found many examples of GFP$^+$ cells in the sensory epithelium expressing Gfi1, which we will refer to as transitioning cells (TC). Overall, there were significantly more TCs in DAPT-treated cristae compared to controls (Fig. 7(C); $t$=4.286, $df$=43, $p$=0.00010). In addition, the number of TCs found in an explant correlated with the degree of *Cre*-mediated recombination in support cells (Fig. 7(D); $r^2$=0.6520, $n$=25, $p$=0.00041). Most DAPT-treated cristae had at least one TC, and in one case there were as many as nine. By contrast, we found only a single TC in all of the DMSO control explants (Fig. 7(D)), which may be a result of spontaneous regeneration as there were no TCs in the 2-day recombination controls.

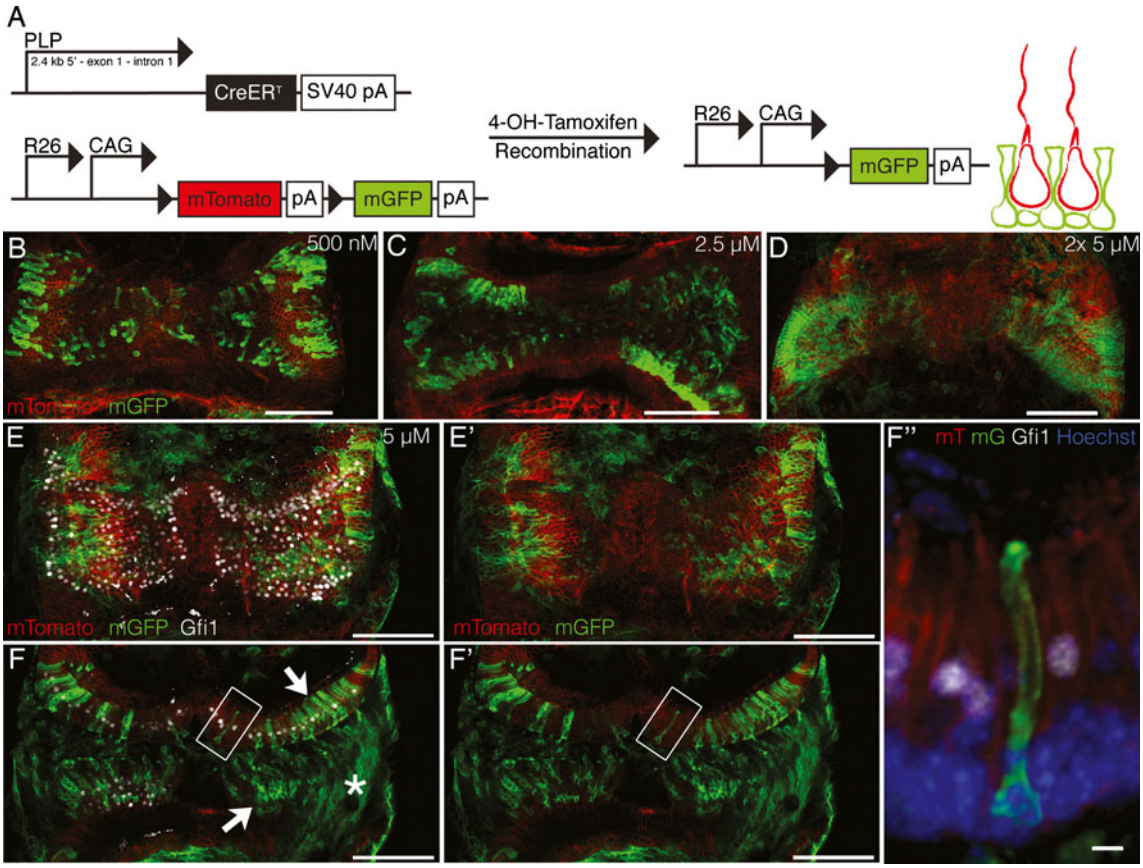


**FIG. 6.** PLP/CreER lineage trace of support cell fate. **A** Mice expressing a tamoxifen-inducible *Cre* recombinase under the PLP promoter were crossed to mTmG reporter mice that express a floxed-stop membrane-bound Tomato followed by a membrane-bound GFP driven by a CAGs promoter in the *ROSA26* locus. **B**,**C**,**D** Tamoxifen-induced recombination was dose dependent. Most support cells in the peripheral region expressed GFP after 2 days of 5 µM 4-OHT treatment with a media change on the second day. **E**,**E′** Fewer support cells expressed GFP after 2 days of 5 µM 4-OHT treatment with no media changes, shown as maximum intensity projections in **E** with Gfi1 (*white*) and in **E′** without Gfi1. **F**,**F′** Single *z* slices of the crista in *E*,*E′* show recombination in support cells (*arrows*) and Schwann cells (*asterisk*). **F″** A zoomed image of the boxed region in *F*,*F′* shows an example of a recombined support cell. All *scale bars* are 100 µm except for in *F″* where it is 5 µm.

The TCs derived from support cells showed a range of morphologies. Most of the TCs were similar to the representative example shown in Figure 8(A,B,C). These cells were found in the hair cell layer and had an immature hair cell morphology including a large, rounded nucleus and longer apical projections than the surrounding GFP$^+$ support cells (arrowhead, Fig. 8(A,B,C)). There were several instances, however, where we observed more intermediate morphologies between that of a support cell and a hair cell. For example, one such cell had an elongated body typical of a support cell but appeared to be lifting off of the basement membrane and in the process of translocating to the hair cell layer (Fig. 8(D,E,F); Supplemental Movie 2 in the ESM). The apical projection of this cell was thinner than the other labeled support cells and it had intense apical mGFP labeling with an appearance unlike other hair cells or support cells (arrowhead in Fig. 8(D,E)). In addition, there were TCs located in the hair cell layer with hair cell morphologies that maintained contact with the basement membrane through thin, foot-like projections (arrowhead, Fig. 8(G,H,I); Supplemental Movie 3 in the ESM). In one instance, we also observed a TC that appeared to have a more mature morphology that was more characteristic of a 'normal' hair cell. This TC was in the hair cell layer with a hair cell appearance, including a large rounded nucleus and a thin apical neck. In addition to having what appears to be a stereocilia bundle like the majority of the TCs, this cell also had a clear kinocilium extending from its apical surface (arrowheads, Fig. 8(J,K,L); Supplemental Movie 4 in the ESM). This was the most mature-looking cell that we observed.

Overall, these data suggest that Notch signaling may play a role in maintaining the support cell phenotype in a subset of support cells in the mature cristae. Upon DAPT-treatment, these support cells can transdifferentiate into hair cells that express the hair cell marker Gfi1, translocate to the hair cell layer,

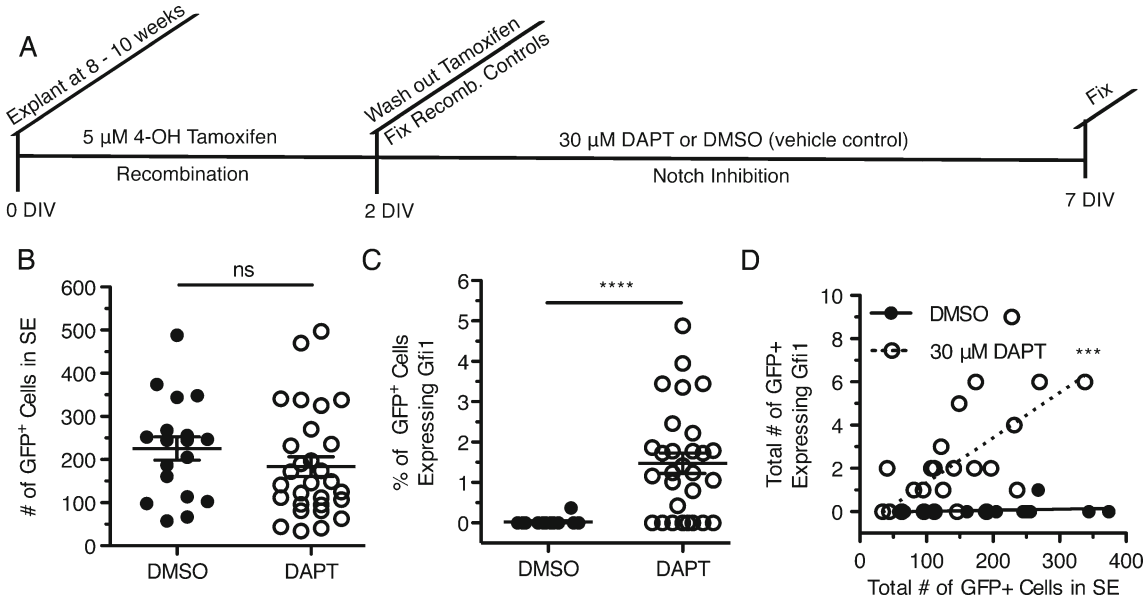


**FIG. 7.** DAPT treatment induced transdifferentiation of support cells to hair cells. **A** Cristae were explanted from 8- to 10-week-old PLP/CreER;mTmG mice and cultured for 2 DIV with a single dose of 5 μm 4-OHT. Recombination control cristae were fixed after 2 days and remaining cristae were washed and treated with either 30 μM DAPT or DMSO for five additional days with daily media changes. **B** The number of $GFP^+$ cells in the sensory epithelium was similar between treatment groups (DMSO—225.6±27.3, $n$=18; DAPT—183.8±22.0, $n$=29) ($t$=1.155, $df$=45, $p$=0.25). *Error bars* depict SEM. **C** There was a significant increase in the percentage of $GFP^+$ cells in the SE expressing Gfi1 in DAPT-treated cristae versus DMSO controls (DMSO—0.023±0.023, $n$=16; DAPT—1.47±0.25, $n$=29) ($t$=4.286, $df$=43, $p$=0.00010). *Error bars* depict SEM. Two-tailed unpaired Student's $t$ test where ns denotes $p>0.05$ and **** denotes $p\leq0.0001$. **D** Overall, in the DAPT-treated cristae the number of $GFP^+$ cells expressing Gfi1 correlated with the recombination efficiency of the explants ($r^2$=0.6520, $n$=25, $p$=0.00041). The DMSO controls showed no significant correlation ($r^2$=0.1873, $n$=16, $p$=0.49). Pearson's correlation where *** denotes $p\leq0.001$.

and take on a hair cell morphology, which in one case included a long kinocilium.

## DISCUSSION

Our results demonstrate that Notch signaling is active in the mature mammalian cristae and may be important for maintaining the support cell fate in a subset of support cells. Culturing postnatal and adult cristae from Hes5-GFP reporter mice with the γ-secretase inhibitor, DAPT, decreased the expression of the Notch effectors *Hes5* and *Hes1*. Hes5, as reported by Hes5-GFP, was downregulated specifically in peripheral support cells. DAPT treatment resulted in an increase in the total number of $Gfi1^+$ hair cells at a similar rate in both the mature and postnatal cristae. New hair cells arose without proliferation, as no hair cells incorporated EdU when it was present throughout the entire culture period. Instead, lineage tracing in adult cristae showed hair cells arose through transdifferentiation of PLP-expressing support cells. These transdifferentiated cells expressed the hair cell marker Gfi1 and were capable of displaying hair cell morphologies, migrating to the correct cell layer, and assembling a stereocilia bundle with a kinocilium.

Previous work in the mature chinchilla cristae provided evidence for spontaneous hair cell regeneration after damage (Tanyeri et al. 1995; Lopez et al. 1997, 1998, 2003). These studies found a partial recovery in hair cell number and innervation over time without a concomitant decrease in support cells. While this was suggestive of proliferative regeneration, the limitations of the chinchilla system prevented further analysis. Here, in addition to providing further evidence for hair cell regeneration in the mature mammalian cristae, we show that hair cells arise through transdifferentiation of support cells using lineage tracing with PLP/CreER;mTmG mice. Though we cannot account for hair cell survival or repair, the use of these mice shows that at least some of our hair cell increases are due to support cell transdifferentiation. Further, though we attribute these increases to Notch inhibition, other pathways could be involved as DAPT inhibits all γ-secretase-processed proteins.

In similar experiments performed by Collado et al. (2011) in the cultured mouse utricle, the ability to generate hair cells with DAPT was lost within the second postnatal week. Other utricle studies suggested that hair cell damage is required for Notch-mediated regeneration in the adult (Wang et al. 2010; Lin et al. 2011; Jung et al. 2013), consistent with what has been shown in the zebrafish lateral line and the

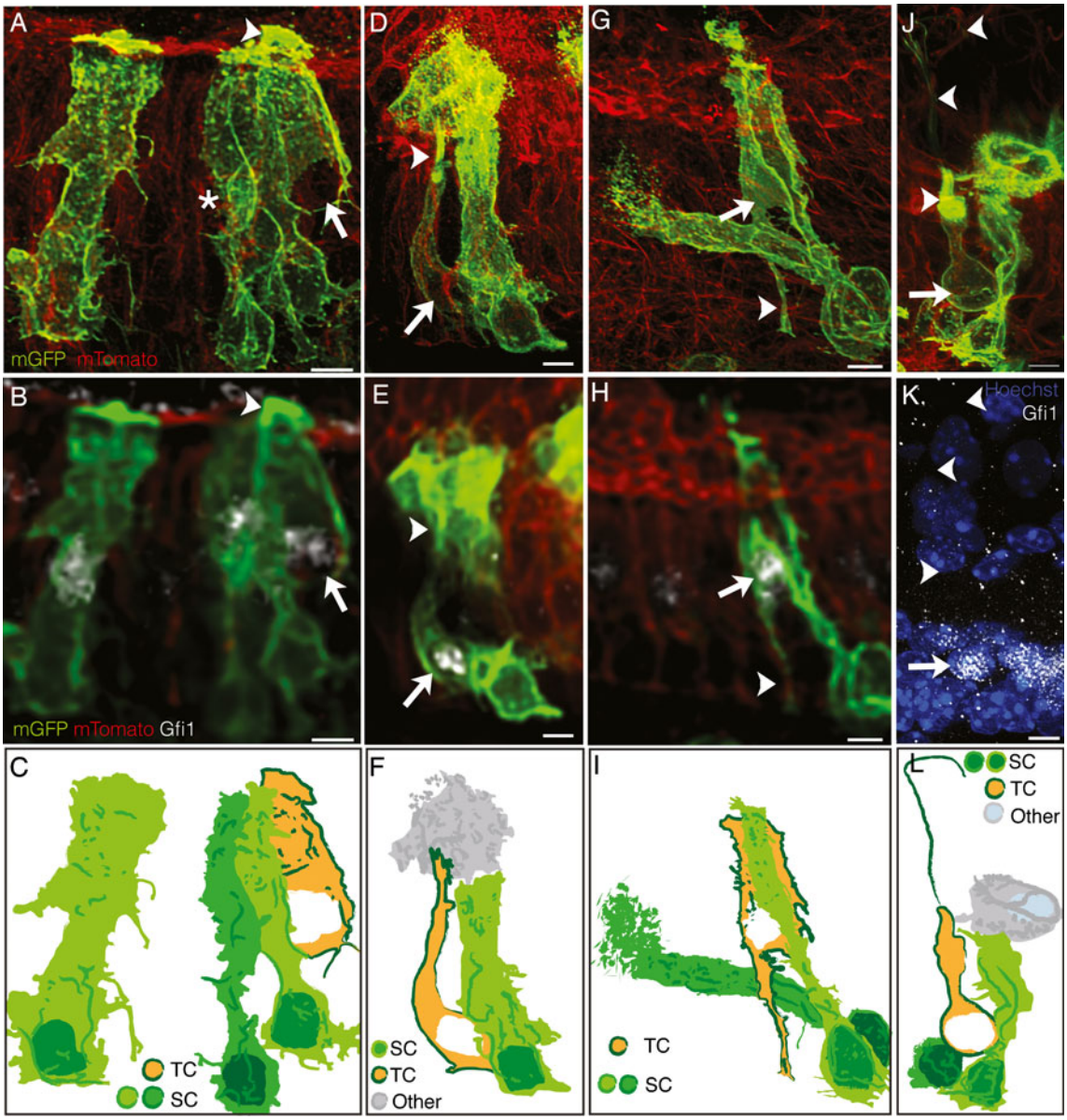


**FIG. 8.** Examples of lineage traced transitional cells (TC). Two views of the cells are shown, one at 60× (**A**,**D**,**G**) and the other at 20× (**B**,**E**,**H**), due to bleaching of the Gfi1 staining at the higher magnification. All *scale bars*, 5 μm. **A**,**B**,**C** An example of a lineage traced cell representative of the majority of observed TCs. This cell was located in the hair cell layer, expressed Gfi1 (*arrow*), and had a taller apical mGFP labeling than surrounding support cells (SC) (*arrowhead*). A diagram of this cell (**C**) also shows several GFP$^+$ support cells near the hair cell, one of which partially enveloped an unlabeled hair cell (*dark green* cell, *asterisk* in **A**). **D**,**E**,**F** A lineage traced cell with a morphology intermediate between a hair cell and a support cell. This cell expressed Gfi1 (*arrow*) and also had a taller apical mGFP labeling (*arrowhead*). This cell, however, was not in the hair cell layer, nor was it attached to the basement membrane. A diagram of this cell (**F**) also shows several GFP$^+$ nonsensory cells (other) and a GFP$^+$ support cell surrounding the TC. **G–I** Another lineage traced TC had a traditional hair cell morphology and Gfi1 expression (*arrow*), but also had a trailing foot attached to the basement membrane (*arrowhead*). A diagram of this cell (**I**) also shows two GFP$^+$ support cells. **J–L** The last example TC had a typical hair cell morphology, a kinocilium (*arrowhead* in **J**), and Gfi1 expression (*arrow* in **K**). A diagram of this cell (**L**) also shows a GFP$^+$ nonsensory cell and two GFP$^+$ support cells surrounding the hair cell.

chick basilar papilla (Ma et al. 2008; Daudet et al. 2009). Due to the damage in our adult cultures, we cannot preclude the possibility that damage is necessary for DAPT-induced hair cell generation. It is also possible that further damage could stimulate additional regeneration.

In our lineage tracing experiments using the PLP/CreER;mTmG mice, we observed several interesting morphological changes in our transdifferentiating cells. These changes were similar to those noted in the initial reports on transdifferentiation in the mature regenerating organs of bullfrogs (Baird et al. 1996;

Steyger et al. 1997), chicks (Raphael et al. 1994; Adler and Raphael 1996; Adler et al. 1997), bats (Kirkegaard and Jorgensen 2000), and guinea pigs (Li and Forge 1997). Since hair cell regeneration occurs in most vertebrate species, it is perhaps unsurprising that these different species show similar changes as cells transition between the distinct morphologies of support cells and hair cells. Most of these studies reported transdifferentiating cells with morphologies intermediate between those of support cells and hair cells. Like support cells, these cells were elongated and spanned the entire sensory epithelium. However, these cells also had enlarged, basally located nuclei and immature stereocilia bundles, suggesting that they were becoming hair cells. In our data, most of the cells appeared to be in later stages of transdifferentiation. Most of our cells had typical hair cell morphologies, were located in the hair cell layer, and appeared to have longer apical processes. However, we observed two types of cells that appeared to be in earlier stages almost identical to those previously reported. The first cell was located near the planum semilunatum and had a transitional morphology between a hair cell and a support cell. Further, this cell was separated from the basement membrane, appearing to be translocating its nucleus to the hair cell layer. This is similar to other studies in the chick basilar papilla where it appeared that detachment from the basement membrane occurred early, prior to or during translocation of the nucleus (Raphael et al. 1994; Adler et al. 1997). The second cell, located near the eminentia cruciatum, had a characteristic hair cell morphology and layering, but maintained contact with the basement membrane through a thin foot-like projection. This is similar to the study by Li and Forge (1997) in the guinea pig utricle where it appeared that transitioning cells maintained contact with the basement membrane until later stages of transdifferentiation. These basal projections are also seen in other cases where hair cells are generated through overexpression of cyclin D1 or Atoh1 (Loponen et al. 2011; Lewis et al. 2012). Though we did not have the same subcellular resolution as the thin sections used in most of these previous experiments, the membrane-bound GFP allowed us to observe nearly identical intermediate morphologies in whole mount explants. Whether these different morphological changes represent distinct mechanisms, it is interesting that support cell transdifferentiation may proceed through similar intermediate morphologies in the chick basilar papilla, the guinea pig utricle, and the mouse cristae.

While the morphological changes occurring during transdifferentiation may be similar between species, the regenerative ability of mammals, whether spontaneous or through manipulations such as Notch inhibition, is much lower than all other vertebrates studied (reviewed in Warchol 2011). This suggests that only a subset of support cells remain competent to form hair cells in the mature mammalian vestibular system. The role for additional factors, such as other signaling pathways or further regulation downstream of Notch signaling is apparent in our data, since only a fraction of the peripheral support cells that express Hes5 and downregulate it in response to Notch inhibition undergo transdifferentiation. However, determining the identity of these factors and why they only affect certain support cells ultimately requires a better understanding of vestibular support cells and their markers. Here, we show that some of the support cells capable of transdifferentiating express the PLP transgene, as was also shown in the postnatal utricle (Collado et al. 2011). In addition, in P7 explants we find that the support cells near the eminentia cruciatum are the most responsive to Notch inhibition. Though there is no obvious difference in Hes5 expression or downregulation in this region, more hair cells were generated here with a concomitant loss in support cells following Notch inhibition. While this regionalization is not apparent in the adult explants, this increase in hair cells at P7 near the eminentia cruciatum is similar to what Lopez et al. (1997) reported in the mature chinchilla cristae. Notably, the eminentia cruciatium is the only region in the crista that expresses the zinc finger gene GATA-3 that is also found in the utricular striola (Karis et al. 2001). This regional GATA-3 expression could be important for hair cell regeneration through downstream signaling targets such as Wnt (Alvarado et al. 2009). In our experiments using mature PLP/CreER;mTmG mice, we found lineage-traced hair cells throughout the peripheral zone of the cristae, both near the eminentia cruciatum and the planum semilunatum. Therefore, while the PLP transgene limited our analysis to the peripheral zone, within this region there was not a particular area of regenerative competence in the adult. In the mature regenerating utricle, there does appear to be regional regeneration (Collado et al. 2011; Lin et al. 2011; Golub et al. 2012; Jung et al. 2013). However, there is no consensus on which regions are competent for regeneration as the regionalization found varied between studies.

Overall, our data provides further evidence that the mammalian cristae, like the other vestibular sensory organs, have the capacity for hair cell regeneration. Since it is currently unknown how many new hair cells would be required to noticeably restore function in a damaged crista, the stimulation of hair cell regeneration by DAPT treatment that we have demonstrated may have some therapeutic relevance (Kopke et al. 2001). Though very promising, the number of hair cells generated here is likely insufficient to fully repair a damaged organ, which is also true of all other mammalian vestibular regeneration to date (Forge et

al. 1993; Warchol et al. 1993; Rubel et al. 1995; Tanyeri et al. 1995; Li and Forge 1997; Lopez et al. 2003; Kawamoto et al. 2009; Lin et al. 2011; Golub et al. 2012; Jung et al. 2013). In order to overcome these limitations on mammalian regeneration, we ultimately need a better understanding of the factors and pathways that mediate hair cell regeneration. Here, we have provided a method for culturing cristae in vitro and have demonstrated that Notch signaling is active in the mature cristae and that DAPT treatment results in hair cell generation through trans-differentiation. This work, therefore, provides the foundation for including the cristae in the future comparative regenerative research that will hopefully further our understanding of how to induce robust hair cell regeneration in mammals.

## ACKNOWLEDGMENTS

This work was supported by the following grants: PHS R21 DC010862 from NIDCD/NIH, PHS NRSA T32 GM07270 from NIGMS/NIH, and PHS P30 DC004661 from NIDCD/NIH. We thank Dr. Byron Hartman for his significant contribution to the development of this work; Dr. Verdon Taylor for the Hes5-GFP mice; Dr. Hugo Bellen for the Gfi1 antibody; Dr. Vidhya Munnamalai for the schematic of the inner ear; Catherine Ray and Katena Koemmpel for technical support; past and present members of the Bermingham-McDonogh, Reh, and Chao labs for helpful discussions; Drs. Thomas Reh, David Raible, Ajay Dhaka, Anna La Torre, and Yumi Ueki for critical comments on the manuscript; the Biology of the Inner Ear Course at the Marine Biological Laboratory for helpful instruction; Dr. Ronald Seifert for help with microscopy; and the Lynn and Mike Garvey Cell Imaging Lab.

## REFERENCES

Adler HJ, Raphael Y (1996) New hair cells arise from supporting cell conversion in the acoustically damaged chick inner ear. Neurosci Lett 205:17–20

Adler HJ, Komeda M, Raphael Y (1997) Further evidence for supporting cell conversion in the damaged avian basilar papilla. Int J Dev Neurosci 15:375–385

Alvarado DM, Veile R, Speck J, Warchol M, Lovett M (2009) Downstream targets of GATA3 in the vestibular sensory organs of the inner ear. Dev Dyn 238:3093–3102

Baird RA, Steyger PS, Schuff NR (1996) Mitotic and nonmitotic hair cell regeneration in the bullfrog vestibular otolith organs. Ann N Y Acad Sci 781:59–70

Basak O, Taylor V (2007) Identification of self-replicating multipotent progenitors in the embryonic nervous system by high Notch activity and Hes5 expression. Eur J Neurosci 25:1006–1022

Collado MS, Thiede BR, Baker W, Askew C, Igbani LM, Corwin JT (2011) The postnatal accumulation of junctional E-cadherin is inversely correlated with the capacity for supporting cells to convert directly into sensory hair cells in mammalian balance organs. J Neurosci 31:11855–11866

Cotanche DA, Kaiser CL (2010) Hair cell fate decisions in cochlear development and regeneration. Hear Res 266:18–25

Daudet N, Gibson R, Shang J, Bernard A, Lewis J, Stone J (2009) Notch regulation of progenitor cell behavior in quiescent and regenerating auditory epithelium of mature birds. Dev Biol 326:86–100

de Moraes SA, Soares WJ, Rodrigues RA, Fett WC, Ferriolli E, Perracini MR (2011) Dizziness in community-dwelling older adults: a population-based study. Braz J Otorhinolaryngol 77:691–699

Desai SS, Zeh C, Lysakowski A (2005a) Comparative morphology of rodent vestibular periphery. I. Saccular and utricular maculae. J Neurophysiol 93:251–266

Desai SS, Ali H, Lysakowski A (2005b) Comparative morphology of rodent vestibular periphery. II. Cristae ampullares. J Neurophysiol 93:267–280

Doerflinger NH, Macklin WB, Popko B (2003) Inducible site-specific recombination in myelinating cells. Genesis 35:63–72

Forge A, Li L, Corwin JT, Nevill G (1993) Ultrastructural evidence for hair cell regeneration in the mammalian inner ear. Science 259:1616–1619

Forge A, Li L, Nevill G (1998) Hair cell recovery in the vestibular sensory epithelia of mature guinea pigs. J Comp Neurol 397:69–88

Fritzsch B, Dillard M, Lavado A, Harvey NL, Jahan I (2010) Canal cristae growth and fiber extension to the outer hair cells of the mouse ear require Prox1 activity. PLoS One 5:e9377

Golub JS, Tong L, Ngyuen TB, Hume CR, Palmiter RD, Rubel EW, Stone JS (2012) Hair cell replacement in adult mouse utricles after targeted ablation of hair cells with diphtheria toxin. J Neurosci 32:15093–15105

Gomez-Casati ME, Murtie J, Taylor B, Corfas G (2010) Cell-specific inducible gene recombination in postnatal inner ear supporting cells and glia. J Assoc Res Otolaryngol 11:19–26

Gopinath B, McMahon CM, Rochtchina E, Mitchell P (2009) Dizziness and vertigo in an older population: the Blue Mountains prospective cross-sectional study. Clin Otolaryngol 34:552–556

Hartman BH, Basak O, Nelson BR, Taylor V, Bermingham-McDonogh O, Reh TA (2009) Hes5 expression in the postnatal and adult mouse inner ear and the drug-damaged cochlea. J Assoc Res Otolaryngol 10:321–340

Hasson T, Heintzelman MB, Santos-Sacchi J, Corey DP, Mooseker MS (1995) Expression in cochlea and retina of myosin VIIa, the gene product defective in Usher syndrome type 1B. Proc Natl Acad Sci U S A 92:9815–9819

Hayashi T, Kokubo H, Hartman BH, Ray CA, Reh TA, Bermingham-McDonogh O (2008) Hesr1 and Hesr2 may act as early effectors of Notch signaling in the developing cochlea. Dev Biol 316:87–99

Hertzano R, Montcouquiol M, Rashi-Elkeles S, Elkon R, Yucel R, Frankel WN, Rechavi G, Moroy T, Friedman TB, Kelley MW, Avraham KB (2004) Transcription profiling of inner ears from Pou4f3(ddl/ddl) identifies Gfi1 as a target of the Pou4f3 deafness gene. Hum Mol Genet 13:2143–2153

Hume CR, Bratt DL, Oesterle EC (2007) Expression of LHX3 and SOX2 during mouse inner ear development. Gene Expr Patterns 7:798–807

Jung JY, Avenarius MR, Adamsky S, Alpert E, Feinstein E, Raphael Y (2013) SiRNA targeting Hes5 augments hair cell regeneration in aminoglycoside-damaged mouse utricle. Mol Ther 21:834–841

Karis A, Pata I, van Doorninck JH, Grosveld F, de Zeeuw CI, de Caprona D, Fritzsch B (2001) Transcription factor GATA-3 alters pathway selection of olivocochlear neurons and affects morphogenesis of the ear. J Comp Neurol 429:615–630

KAWAMOTO K, IZUMIKAWA M, BEYER LA, ATKIN GM, RAPHAEL Y (2009) Spontaneous hair cell regeneration in the mouse utricle following gentamicin ototoxicity. Hear Res 247:17–26

KIERNAN AE (2006) The paintfill method as a tool for analyzing the three-dimensional structure of the inner ear. Brain Res 1091:270–276

KIRKEGAARD M, JORGENSEN JM (2000) Continuous hair cell turnover in the inner ear vestibular organs of a mammal, the Daubenton's bat (*Myotis daubentonii*). Naturwissenschaften 87:83–86

KOPKE RD, JACKSON RL, LI G, RASMUSSEN MD, HOFFER ME, FRENZ DA, COSTELLO M, SCHULTHEISS P, VAN DE WATER TR (2001) Growth factor treatment enhances vestibular hair cell renewal and results in improved vestibular function. Proc Natl Acad Sci U S A 98:5886–5891

KROENKE K, HOFFMAN RM, EINSTADTER D (2000) How common are various causes of dizziness? A critical review. South Med J 93:160–167, quiz 168

LEWIS RM, HUME CR, STONE JS (2012) Atoh1 expression and function during auditory hair cell regeneration in post-hatch chickens. Hear Res 289:74–85

LI L, FORGE A (1997) Morphological evidence for supporting cell to hair cell conversion in the mammalian utricular macula. Int J Dev Neurosci 15:433–446

LIN V, GOLUB JS, NGUYEN TB, HUME CR, OESTERLE EC, STONE JS (2011) Inhibition of Notch activity promotes nonmitotic regeneration of hair cells in the adult mouse utricles. J Neurosci 31:15329–15339

LOPEZ I, HONRUBIA V, LEE SC, SCHOEMAN G, BEYKIRCH K (1997) Quantification of the process of hair cell loss and recovery in the chinchilla crista ampullaris after gentamicin treatment. Int J Dev Neurosci 15:447–461

LOPEZ I, HONRUBIA V, LEE SC, LI G, BEYKIRCH K (1998) Hair cell recovery in the chinchilla crista ampullaris after gentamicin treatment: a quantitative approach. Otolaryngol Head Neck Surg 119:255–262

LOPEZ I, AYALA C, HONRUBIA V (2003) Synaptophysin immunohistochemistry during vestibular hair cell recovery after gentamicin treatment. Audiol Neurootol 8:80–90

LOPONEN H, YLIKOSKI J, ALBRECHT JH, PIRVOLA U (2011) Restrictions in cell cycle progression of adult vestibular supporting cells in response to ectopic cyclin D1 expression. PLoS One 6:e27360

MA EY, RUBEL EW, RAIBLE DW (2008) Notch signaling regulates the extent of hair cell regeneration in the zebrafish lateral line. J Neurosci 28:2261–2273

MENDEL B, BERGENIUS J, LANGIUS-EKLOF A (2010) Dizziness: a common, troublesome symptom but often treatable. J Vestib Res 20:391–398

MORSLI H, CHOO D, RYAN A, JOHNSON R, WU DK (1998) Development of the mouse inner ear and origin of its sensory organs. J Neurosci 18:3327–3335

MUZUMDAR MD, TASIC B, MIYAMICHI K, LI L, LUO L (2007) A global double-fluorescent Cre reporter mouse. Genesis 45:593–605

NEUHAUSER HK, RADTKE A, VON BREVERN M, LEZIUS F, FELDMANN M, LEMPERT T (2008) Burden of dizziness and vertigo in the community. Arch Intern Med 168:2118–2124

OESTERLE EC, CAMPBELL S, TAYLOR RR, FORGE A, HUME CR (2008) Sox2 and JAGGED1 expression in normal and drug-damaged adult mouse inner ear. J Assoc Res Otolaryngol 9:65–89

RAPHAEL Y, ADLER HJ, WANG Y, FINGER PA (1994) Cell cycle of transdifferentiating supporting cells in the basilar papilla. Hear Res 80:53–63

RUBEL EW, DEW LA, ROBERSON DW (1995) Mammalian vestibular hair cell regeneration. Science 267:701–707

STEYGER PS, BURTON M, HAWKINS JR, SCHUFF NR, BAIRD RA (1997) Calbindin and parvalbumin are early markers of non-mitotically regenerating hair cells in the bullfrog vestibular otolith organs. Int J Dev Neurosci 15:417–432

TANYERI H, LOPEZ I, HONRUBIA V (1995) Histological evidence for hair cell regeneration after ototoxic cell destruction with local application of gentamicin in the chinchilla crista ampullaris. Hear Res 89:194–202

WALLIS D, HAMBLEN M, ZHOU Y, VENKEN KJ, SCHUMACHER A, GRIMES HL, ZOGHBI HY, ORKIN SH, BELLEN HJ (2003) The zinc finger transcription factor Gfi1, implicated in lymphomagenesis, is required for inner ear hair cell differentiation and survival. Development 130:221–232

WANG GP, CHATTERJEE I, BATTS SA, WONG HT, GONG TW, GONG SS, RAPHAEL Y (2010) Notch signaling and Atoh1 expression during hair cell regeneration in the mouse utricle. Hear Res 267:61–70

WARCHOL ME (2011) Sensory regeneration in the vertebrate inner ear: differences at the levels of cells and species. Hear Res 273:72–79

WARCHOL ME, LAMBERT PR, GOLDSTEIN BJ, FORGE A, CORWIN JT (1993) Regenerative proliferation in inner ear sensory epithelia from adult guinea pigs and humans. Science 259:1619–1622

YANG H, GAN J, XIE X, DENG M, FENG L, CHEN X, GAO Z, GAN L (2010) Gfi1-Cre knock-in mouse line: a tool for inner ear hair cell-specific gene deletion. Genesis 48:400–406

ZHENG JL, SHOU J, GUILLEMOT F, KAGEYAMA R, GAO WQ (2000) Hes1 is a negative regulator of inner ear hair cell differentiation. Development 127:4551–4560

ZINE A, AUBERT A, QIU J, THERIANOS S, GUILLEMOT F, KAGEYAMA R, DE RIBAUPIERRE F (2001) Hes1 and Hes5 activities are required for the normal development of the hair cells in the mammalian inner ear. J Neurosci 21:4712–4720